La mer 56 : 21–35, 2018
Société franco-japonaise d'océanographie, Tokyo

Individual-level variability in the behavioral responses of female *Oithona davisae* (Copepoda: Cyclopoida) to hydromechanical stimuli

Baobo LIU[1)], Tatsuro AKIBA[2)]*, José María LANDEIRA[1)] and Yuji TANAKA[1)]

Abstract: Planktonic copepods can detect potential preys and predators through mechanoreception. Sensing a certain level of deformation rate of ambient water, they escape from the source of stimulus. Quantification of the deformation rates that evoke the escape behavior of copepods may thus help understand their living strategies. The term "zooplankton" generally refers to assemblages of individual zooplankters, and "zooplankton" has been usually studied by ignoring inter-individual differences. We here observed and quantified individually the behaviors of female *Oithona davisae* under spatially changing deformation rates produced with a suction flow system. Female *O. davisae* typically escaped after being drawn to areas with deformation rates ranging 0.1–1.9 (0.54 ± 0.45) s^{-1}. To escape, they jumped towards lower-deformation conditions with higher speed and longer distance than without stimulus, showing that they can detect not only the strength but also the directional information of flow fields. Moreover, significant inter-individual differences in the behavior were observed, indicating that copepods are a group of organisms with different individual characteristics. Our results also suggest that female *O. davisae* prefers to stay in a quiescent environment where local deformation rate is smaller than 0.1 s^{-1}. Because female *O. davisae* ambushes prey by detecting weak hydromechanical signals, staying in environments with lower deformation rates may be beneficial to detect prey.

Keywords : *Oithona davisae, behavioral response, hydromechanical stimulus, inter-individual difference*

1) Graduate School of Marine Science and Technology, Tokyo University of Marine Science and Technology, 4–5–7 Konan, Minato-ku, Tokyo 108–8477, Japan
2) National Institute of Advanced Industrial Science and Technology, 1–1–1 Higashi, Tsukuba, Ibaraki 305–8565, Japan
* Corresponding author:
Tel: + 81–29–861–6703
Fax: + 81–29–861–3048
E-mail: ta-akiba@aist.go.jp

Introduction

Planktonic copepods can locate potential preys, predators, and mates remotely through mechanoreception (YEN *et al.*, 1992; FIELDS *et al.*, 2002). Armed with mechanoreceptory setae on many of their appendages (especially the first antennae), they can detect low hydromechanical stimuli, and respond rapidly in the aquatic environment (KIØRBOE and VISSER, 1999; LENZ and HARTLINE, 1999; VISSER 2001; FIELDS *et al.*, 2012). Therefore, the characterization and quantifica-

tion of the behavioral responses of copepods to hydromechanical stimuli allow us to understand better their foraging, predator avoidance, and reproduction strategies (JIANG and OSBORN, 2004).

A velocity gradient in the ambient water can bend the setae of copepods, and subsequently triggers their behavioral responses (STRICKLER and BAL, 1973). Among all components of velocity gradients, copepods respond specifically to the deformation (*i.e.* rate of strain) (FIELDS and YEN, 1997; KIØRBOE *et al*., 1999). To quantify the deformation rates that trigger copepods to escape, the responses of copepods have been examined in suction flows generated by gravity-forced draining of water (FIELDS and YEN, 1997; KIØRBOE *et al*., 1999; WAGGETT and BUSKEY, 2007) or peristaltic pumps (BURDICK *et al*., 2007). Due to the mechanism of rotor, suction flow generated by peristaltic pumps sometimes fluctuates. However, gravity-forced draining of water through a submerged suction tube can ideally generate a stable flow field with spatially changing deformation rates in the experimental vessel (KIØRBOE *et al*., 1999; JAKOBSEN, 2001). The deformation rate can be determined by the distance to the suction mouth. Therefore, we used this technique to study copepods' behavioral responses against hydromechanical stimuli quantitatively (KIØRBOE *et al*., 1999; WAGGETT and BUSKEY, 2007; FIELDS *et al*., 2012).

Previous studies have quantified the hydromechanical stimuli required to evoke copepods' escape behavior. Deformation rates on the order of 1–10 s^{-1} trigger escape behaviors in a large variety of copepods (KIØRBOE, 2013; WOODSON *et al*., 2014; VAN SOMMEREN GRÉVE *et al*., 2017). Thresholds of deformation rates have been used to compare the hydromechanical signal levels that trigger the escapes of various copepods (FIELDS and YEN, 1997; KIØRBOE *et al*., 1999; BURDICK *et al*., 2007). In the present study, we aim to quantify the hydromechanical signal that evokes escape behavior of a small-sized cyclopoid copepod, *Oithona davisae*. This species is one of the most dominant zooplankton organisms in coastal and estuarine environments (UYE and SANO, 1995; CEBALLOS and KIØRBOE, 2011), and plays an important trophic role linking primary producers to higher levels of the food web (FERRARI and ORSI, 1984; UYE and SANO, 1995; SAIZ *et al*., 2003). In these environments, adult males of *O. davisae* are outnumbered by females (UYE and SANO, 1995).

Zooplankton generally refers to assemblages of individual zooplankters, and their behaviors are commonly treated as ecologically equivalent among conspecific individuals, and are quantified at species level through combining the data of many individuals together, regardless of the individual (KIØRBOE *et al*., 1999; FIELDS, 2000; BURDICK *et al*., 2007). Thus, behavioral responses of copepods have been traditionally observed with a number of individuals together in a vessel (KIØRBOE *et al*., 1999; FIELDS, 2000; BURDICK *et al*., 2007). However, it is unclear whether copepods of the same species and similar size exhibit similar behavioral responses. In this sense, the swimming behaviors of copepods were observed at individual level.

Through the behavioral observation of the same individual, the present study investigates how female *O. davisae* responds to hydromechanical stimulus. At first, we observed free swimming behaviors of female *O. davisae* in still water. Successively, we generated a spatially-changing suction flow field, and observed its escape behaviors. To observe inter-individual variation in behavioral responses, only one individual was introduced into an experimental vessel. The swimming characteristics both with and without hydromechanical stimuli were quantified from the video sequences.

Materials and methods

Copepod collection, identification, and maintenance

Oithona davisae were collected with a plankton net of 100 μm mesh at the pier of the Shinagawa Campus of Tokyo University of Marine Science and Technology (innermost part of Tokyo Bay). Female adults were isolated from the samples and kept in a 3 L container (salinity of 24) and maintained at 20 ℃ with *Tetraselmis tetrathele* (Prasinophyceae, density of 4×10^3 cells mL^{-1}) as prey. Both culture temperature and water salinity were the same as the conditions in sampling area. Before each observation, an active and undamaged individual was picked out under a stereomicroscope (Olympus SZX7) and photographed with a 5-mega pixel digital color camera (Olympus DP25) (Fig. 1). Size of each copepod was measured using ImageJ software (http://rsb.info.nih.gov/ij/). The copepod was then introduced in the experimental vessel for 1 h of acclimation. We observed in total 8 individuals of similar size (total body length of 410 ± 30 μm, mean ± SD), and without egg sacs.

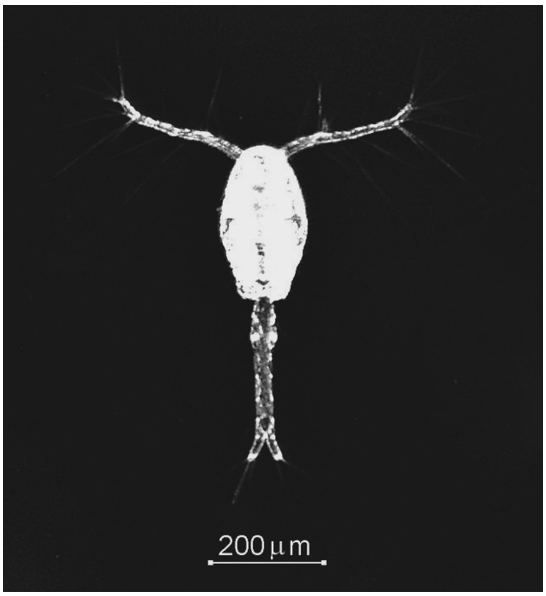

Fig. 1 Female *O. davisae* armed with well-developed mechanoreceptory setae on the first antennae.

Experimental setup

An experimental setup was developed to generate a stable flow field where the deformation rate can be estimated accurately (Fig. 2). The flow field was generated by gravity-forced draining of seawater from a glass pipe (inner diameter of 0.9 mm, outer diameter of 1.1 mm) mounted 20 mm above the bottom of a cubic acrylic vessel (Fig. 2, vessel 1, 70 × 70 × 70 mm). The vessel was filled with 300 mL of filtered seawater (0.7 μm sieve). Salinity of the seawater was 24, and the temperature was 20 ℃ (density of 1.02 g mL^{-1}). A volume flow rate of 3.2 mL min^{-1} was set by adjusting the height of the tube outlet. To keep the suction flow rate constant, water flowing out through the pipe was returned to another vessel (Fig. 2, vessel 2, 70 × 70 × 70 mm) at a same flow rate via a peristaltic pump (MasterFlex 7523-30). Two vessels were connected by a U-shape tube (inner diameter of 12.5 mm, outer diameter of 15 mm), which maintained a constant water level and head pressure over the suction mouth. Owning to the large cross-section area of the U-shape tube, flow speed (mm s^{-1}) of the returning flow was kept only 0.5% of that at suction mouth. Both vessels were covered with a piece of aluminum foil to prevent water evaporation during a long observation.

Flow field

The spatial pattern of the flow field was determined by observing the movements of neutrally buoyant ion exchange resin particles (Diaion SP 20ss, diameter of 40-70 μm, density of 1.01 g mL^{-1}) entrained into the suction flow. Two perpendicularly mounted high-speed cameras (Pho-

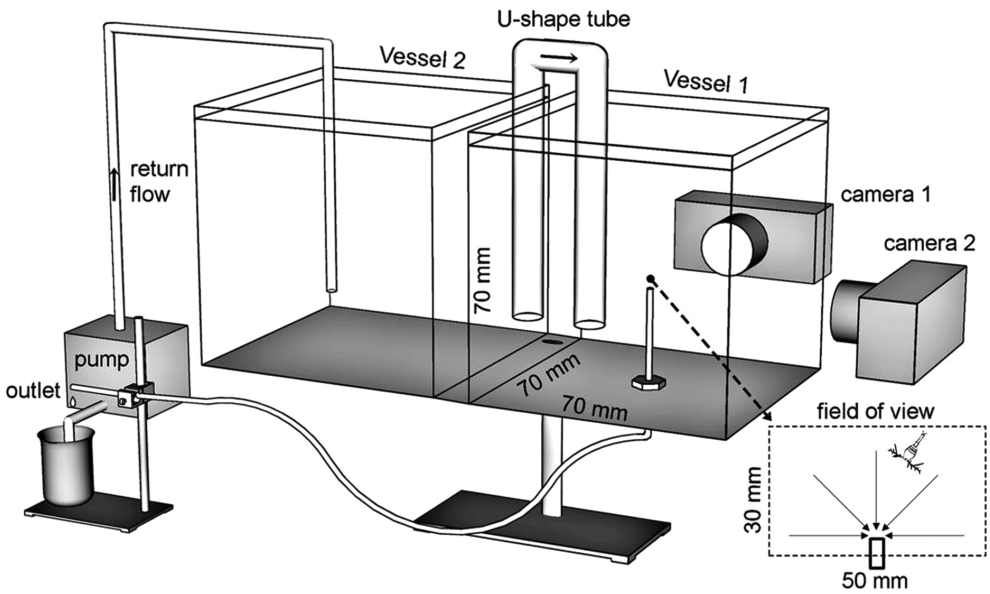

Fig. 2 Experimental setup. A stable suction flow was generated by gravity-forced draining of seawater from a glass pipe (0.9 mm inner-diameter) mounted 20 mm above the bottom of a cubic vessel. The volume flow rate was adjusted to 3.2 mL min^{-1} by changing the height of the outlet. Seawater out of the pipe was returned to another vessel at a same flow rate via a peristaltic pump. Two vessels are connected by a U-shape tube to maintain a constant head pressure over the tube. Swimming behaviors of copepod were observed three-dimensionally with two orthogonally arranged video recorders.

tron 1024PCI, 1000 frames s^{-1}) equipped with a lens (Nikon Micro-Nikkor, 105 mm) were used to record the particle trajectories three-dimensionally. Trajectories of about 60 particles were recorded to analyze the flow field.

When the flow rate is quite slow, and diameter of a suction tube is much smaller than the distance from the copepod to the suction mouth, water motion towards the suction mouth is considered as point-symmetrical potential flow. Continuity demands that the flux through concentric spherical surfaces of various radii (r, mm), with the suction mouth as the center, must be equal to each other, and equal to the volume flow rate (Q, mm^3 s^{-1}). The radially directed flow speed (v, mm s^{-1}) thus equals volume flow rate divided by the surface area of a sphere:

$$v=\frac{Q}{4\pi r^2} \quad (1).$$

The deformation (Δ, s^{-1}) along flow can be quantified as:

$$\Delta=\frac{dv}{dr}=\frac{Q}{2\pi r^3} \quad (2).$$

Within the suction flow, trajectories of particles were radially symmetrical and approximately linear in a range of 1 to 5 mm to the center of the suction mouth (Fig. 3a). Via high-speed imaging, it was observed that the particles were entrained smoothly without any fluctuation (Fig. 3a). And the volume flow rate varied less than 0.1% in 5 hours. We thus confirmed the suction flow to be stable both in short- and long-time.

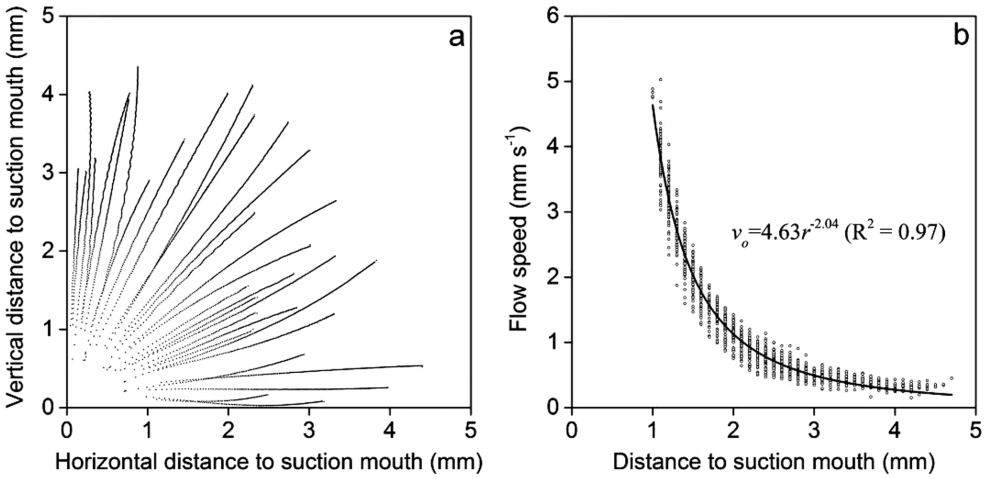

Fig. 3 Flow field above the suction mouth. a. Three-dimensional pathlines of particles above the suction mouth (horizontal distance $=\sqrt{x^2+y^2}$; vertical distance = z). To show the trajectories clearly, tracking data of half of the particles were plotted in the figure. Each dot line represents the trajectory of one particle over time. The dots indicate the positions of the particles at time interval of 20 ms. b. Flow speed values (mm s^{-1}) as a function of distance to the center of suction mouth. The data were selected at equal distance interval of 0.1 mm.

The observed flow speed (v_o, mm s^{-1}) varied almost inversely with the square of distance to the suction mouth (Fig. 3b). The speed and direction both were in small callibration errors (7% and 3.5% respectively) with an ideal condition. Symmetricity was also confirmed in the correlation between flow speed and distance to suction mouth. The deformation rate at any position is thus determined by the relative distance to suction mouth:

$$\Delta = \frac{dv_o}{dr} = 9.45r^{-3.04} \quad (3).$$

Behavioral observations

The behavior of female *O. davisae* was observed three-dimensionally with two orthogonally arranged video recorders (HDR-SR12, 30 frames s^{-1}, 1440 × 1080 pixels), each equipped with a lens (Marumi, 49 mm, MC + 3). The recorders were started simultaneously via a remote controller. The observation volume was 75 mL (50 × 50 × 30 mm) around the pipe mouth with an image resolution of 35 μm $pixel^{-1}$. All experiments were conducted under dark condition to avoid any photic effect on copepods. Two near-infrared light-emitting diodes (LEDs, wavelength of 730 nm) were employed as illumination because copepods are insensitive to near-infrared light (Buskey *et al.*, 1989). LEDs were placed in the opposite directions of 2 lenses, emitting collimated light beams through the vessels into each camera.

The swimming behavior of female *O. davisae* was firstly observed without any stimulus as a control, and subsequently under a stable hydromechanical stimulus. To avoid potential foraging behavioral responses, no food was added into the vessel. To follow the same individual for a long time and test inter-individual variation in behavior, we introduced only one individual into the vessel. Swimming behavior in still water was firstly observed for 50 s, and later, a stable suc-

tion flow was generated. The behavior under hydromechanical stimulus of each replicate was recorded for a long time (5 h). All recorded video data were decoded into image sequences by a video editing software (Grass Valley EDIUS), and the behavioral responses against suction flow were picked out for tracking. We analyzed tracks for 50 s after copepods were placed in the suction flow area.

Image processing and behavioral analysis

Instantaneous coordinates of copepods were digitized with the image processing software (Swallow Series image processing system, DigiMo) of Particle Tracking Velocimetry (PTV). The center of suction mouth was set as the origin in x, y, z coordinates. By combing the position data from both cameras, copepods' swimming trajectories were measured three-dimensionally.

The jump behavior was characterized using the intensity and direction of jump. Jump distance was the total distance travelled along the jump trajectory (time interval of 33.3 ms). Jump speed was the average swimming speed within a jump. The peak acceleration rate was the maximum acceleration rate calculated at a time interval of 33.3 ms. Jump direction in still water was represented as the angle between jump trajectory and gravity direction, while the escape direction was quantified as the angle between jump trajectory and flow direction at initial escape location.

Statistical analysis

Jump without hydromechanical stimulus was defined as a normal jump, while the jump against suction flow was defined as an escape jump. The data for jump characteristics (both normal and escape jump) and deformation rates required to trigger escapes were not normally distributed (Shapiro-Wilk test, $p < 0.05$). Because of the non-normal distribution and unequal variances, the inter-individual differences were analyzed using the nonparametric test Kruskal-Wallis ANOVA, whereas the intra-individual differences between "still water" and "suction flow" conditions were tested with the non-parametric Mann-Whitney ranked sum test. Then, parameters of jump distance, duration, speed, peak acceleration, and direction of both normal and escape jumps, as well as the deformation rate to trigger escape jumps (extracted from 50 s of recording) were compared. Using Kruskal-Wallis ANOVA, the equality of medians of each jump parameter among 8 individuals was tested. The Mann-Whitney ranked sum test was done to evaluate whether normal and escape jump parameters of the same individual were different to each other.

Results

Swimming patterns

In absence of hydromechanical stimuli, female *O. davisae* exhibited characteristic sink-jump behavior (Fig. 4a). For 90–98% (94.9 ± 1.6%) of time, female *O. davisae* sank slowly at speed of 0.25–0.54 (0.37 ± 0.10) mm s^{-1}. The sinking speed varied significantly between individuals (−30% to + 50%). Intermittently, it repositioned its body through short spontaneous jumps at a frequency of 0.3–0.9 (0.5 ± 0.2) times s^{-1}. The jump frequency also showed high inter-individual differences (up to 3 times). In comparison with still water conditions, all individuals performed different behavioral responses against suction flow (Fig. 4b). After the suction flow was started, copepods were sucked towards the mouth of the pipe for the first time. At certain distances to the suction mouth, female *O. davisae* escaped to locate itself far from the suction mouth. The copepod was sucked again when the

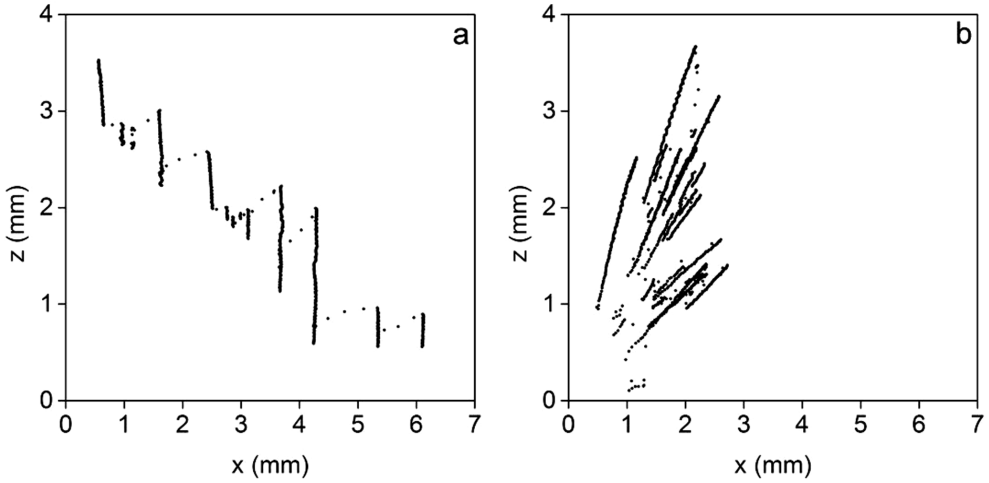

Fig. 4 Two-dimensional swimming trajectories of one individual under "still water" (a) and "suction flow" (b) conditions. Time lengths of the trajectories were all 50 s. Time interval between consequent dots was 33.3 ms. The origin in figure b represents the center of suction mouth.

escape jump finished, and it would initiate another jump.

Hydromechanical signal levels to trigger escape jumps

Jumps were, in all cases, distinguished by rapid changes in swimming speed over time. From the distance between escape position and the center of suction mouth (reaction distance), the deformation rate that triggered escape jumps of female *O. davisae* was calculated with equation 3. They initiated escape jumps at distances of 1.2–5.7 mm to suction mouth where deformation rates ranged from 0.05 to 5.91 s^{-1}. Therefore, female *O. davisae* can respond to a certain range of hydromechanical stimuli. Typically, 90% of escape jumps were triggered at deformation rates of 0.1–1.9 (0.54 ± 0.45) s^{-1}. Moreover, significant inter-individual differences ($p < 0.01$) in the deformation rates that trigger escape jumps were observed (Fig. 5). Compared with the mean value for all individuals (0.88 s^{-1}), the average deformation rate to trigger escapes of each individual varied from -70% to + 95%.

Jump kinematics

The parameters that characterize the swimming behavior were measured in still water and under suction flow (Fig. 6). Overall, in absence of hydromechanical stimuli, adult female *O. davisae* jumped 0.17–0.44 (0.29 ± 0.10) mm in 0.07–0.27 (0.11 ± 0.05) s, with average speeds of 2.0–3.1 (2.4 ± 0.4) mm s^{-1}, and peak accelerations of 70–130 (100 ± 25) mm s^{-2}. In still water, the differences in the parameters jump distance and speed were not statistically significant between individuals ($p > 0.05$), while jump duration and peak acceleration rate varied significantly ($p < 0.01$). Compared with the mean values obtained by combining all individuals together, the average jump duration and peak acceleration of each individual varied from -20% to + 40% and -30% to + 30%, respectively.

Under "suction flow" conditions, female *O. da-*

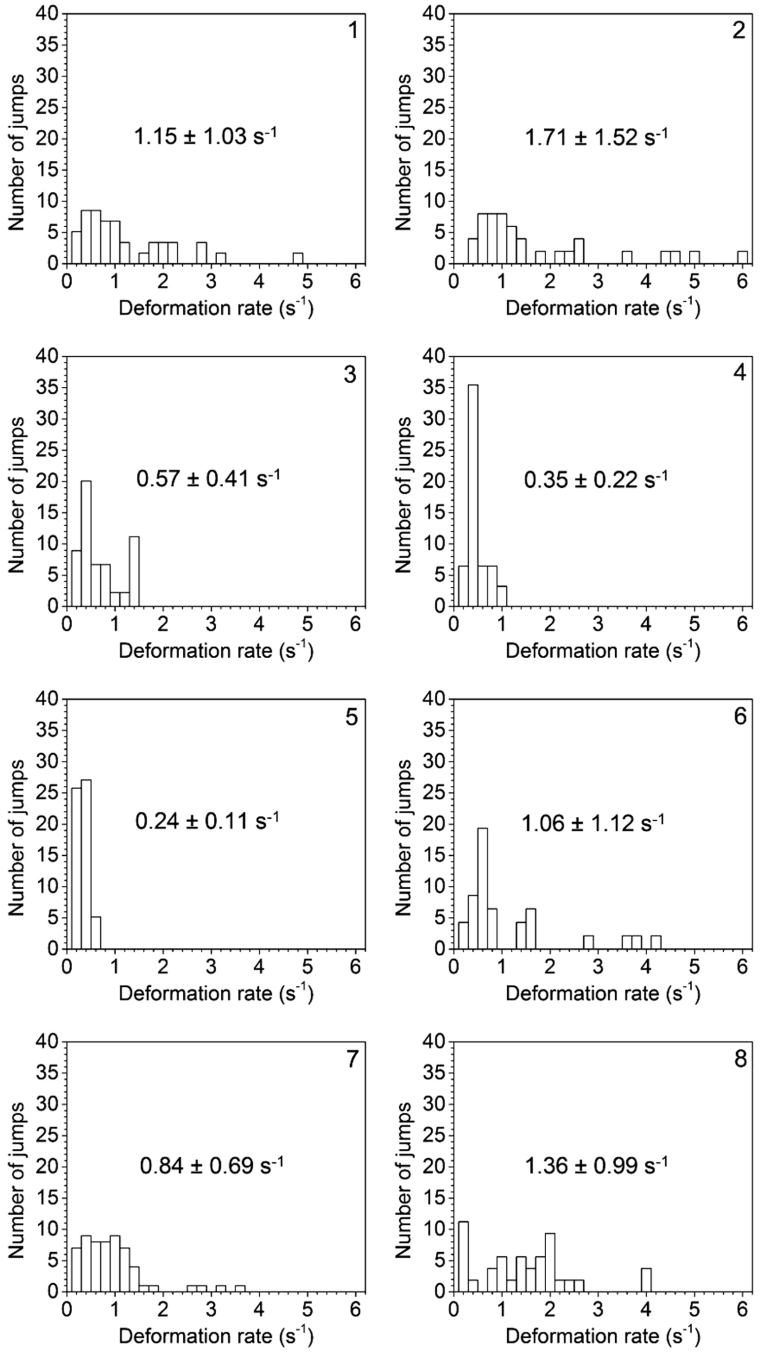

Fig. 5 Distributions of deformation rates that triggered escape jumps of different individuals. The code number of copepod indicates the time order of observation. To avoid bias caused by the unbalance in the number of escape jumps, the total number of escape jumps was modified to be the same (n = 58) for all individuals. Mean deformation rate for all individuals was 0.88 s^{-1}.

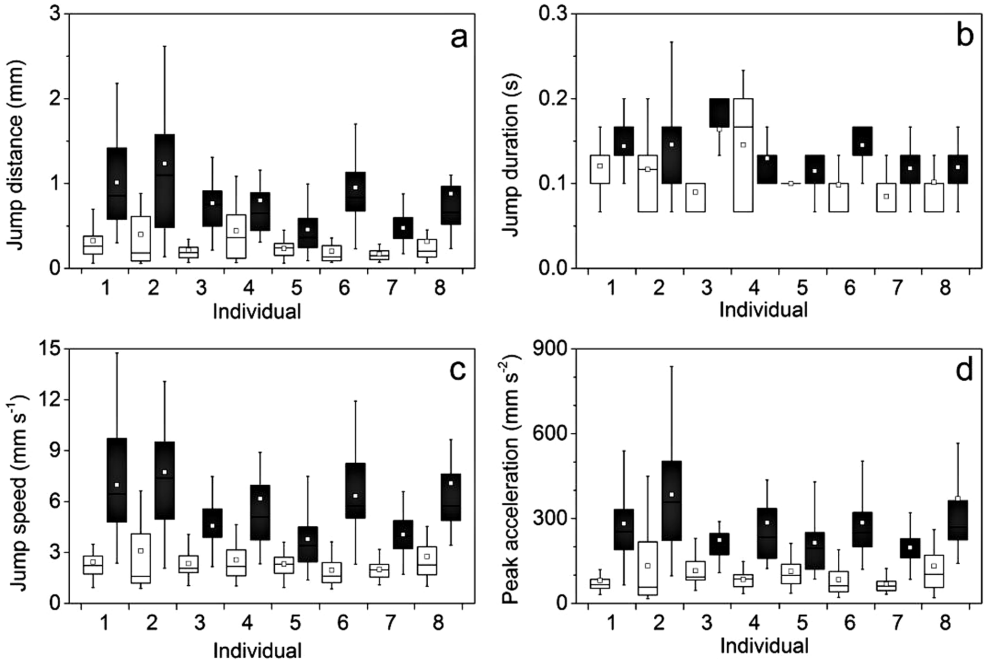

Fig. 6 Jump characteristics of female *O. davisae* under "still water" (white box) and "suction flow" (grey box) conditions. The code number of copepod indicates the time order of observation. Ends of boxes: 25% and 75%; ends of whiskers: 1% and 99% of the data; middle horizontal lines: medians; open squares: mean values.

visae jumped longer distances of 0.46–1.24 (0.82 ± 0.26) mm in 0.07–0.27 (0.13 ± 0.04) s, with speed values of 3.8–7.7 (5.8 ± 1.5) mm s^{-1}, and peak accelerations of 200–390 (280 ± 70) mm s^{-2}. Against suction flow, all jump parameters were significantly different ($p < 0.01$) between individuals. Compared with the mean values for all individuals, the average jump distance, duration, speed, and peak acceleration of each individual varied from −40% to + 50%, −20% to + 20%, −40% to + 30%, and −30% to + 40%, respectively. According to these results, jump characteristics were analyzed individually. By sensing hydromechanical stimuli, female *O. davisae* jumped significantly longer and faster than without stimulus ($p < 0.01$).

Jump direction

We quantified the jump directions of female *O. davisae* against the suction flow and in still water (Fig. 7). In still water, the jump directions showed a random pattern (Fig. 7a). In the suction flow condition, they escaped in directions with angles of 82–178° (139 ± 21°) from flow directions, and 97% of escape jumps were oriented in the opposite direction of the suction flow (Fig. 7b). Thus, female *O. davisae* jumps directionally towards lower-deformation conditions. In addition, jump directions of female *O. davisae* varied significantly between individuals both in "still water" and "suction flow" conditions ($p < 0.001$). Compared with the mean jump angle for all individuals, the average jump direction of each individual varied from −60% to + 80% in still water (mean = 80°) and ± 10% against

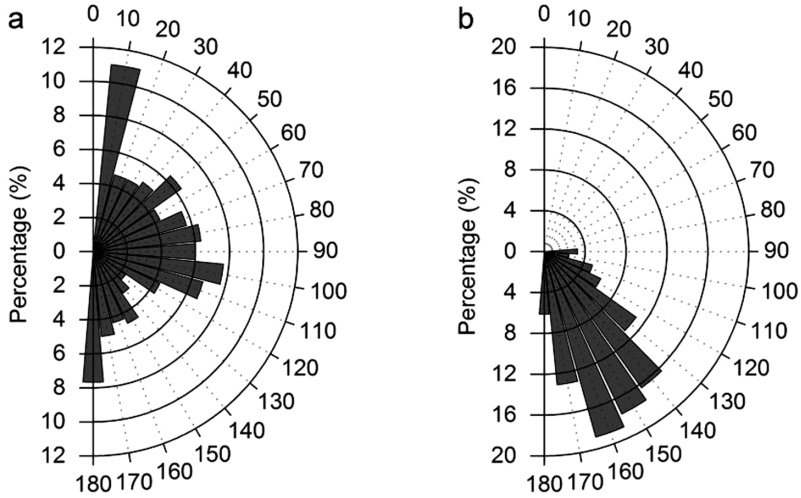

Fig. 7 Wind-rose distributions in jump directions under "still water" (a, n = 193) and "suction flow" (b, n = 266) conditions for all 8 individuals. The jump direction in still water was represented by the angle between jump trajectory (linear connection between initial and terminal points of a jump) and gravity direction (0°). Angles over 90° indicates upward jumps. The jump direction against hydromechanical stimulus was quantified as the angle between jump trajectory and flow direction (0°) at initial escape position. Angle over 90° indicates opposite jump direction from flow direction.

suction flow (mean = 140°), respectively.

Discussions

Behavioral quantification

We studied the behavioral responses of individual female *O. davisae* under a stable "suction flow" condition. Although the hydromechanical stimulus in our study is not the same as flow patterns generated by real predators (which usually change spatio-temporally), we observed that female *O. davisae* initiated escape jumps under certain range of deformation rates. The observed behavioral responses reflect their evolved escape abilities in nature. By combining those quantified escape abilities with real hydromechanical stimuli generated by potential predators, we can evaluate the potential survival rates of female *O. davisae* when encountering a given predator. Therefore, the quantification of the hydromechanical detection ability and swimming ability of copepods may offer important data to explore predator-prey interactions in marine ecosystems (Fields and Yen, 1997).

Hydromechanical signal level

Copepods can sense fluid mechanical signals in a wide range (Strickler and Bal, 1973; Fields *et al*., 2012). Female *O. davisae* typically escaped at positions where deformation rates ranged from 0.1 to 1.9 s^{-1} (0.54 ± 0.45 s^{-1}), which partially (0.1–1 s^{-1}) falls out of the empirical range reported in proceeding works (an order of 1–10 s^{-1}) (Kiørboe, 2013). Compared with other copepods studied by suction flow, female *O. davisae* jumped at relatively lower deformation rates (Fig. 8). This result is consistent with previous observa-

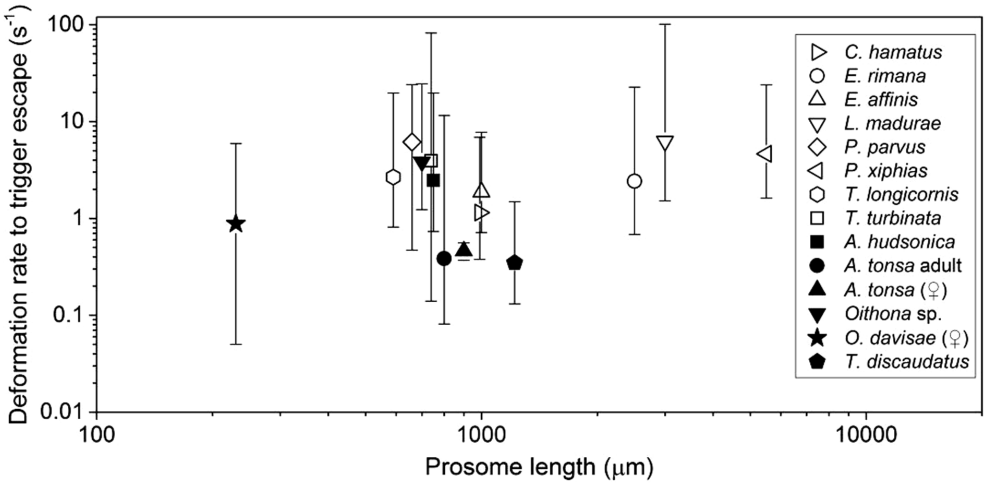

Fig. 8 Summary of hydromechanical signal levels that trigger escape behaviors of a variety of copepods. The deformation rates were all calculated from equation 2 based on the reported reaction distances and volume flow rates in the literature (FIELDS and YEN, 1997; VIITASALO *et al*., 1998; KIØRBOE *et al*., 1999; BURDICK *et al*., 2007; WAGGETT and BUSKEY, 2007). The average deformation rate to trigger escapes was not significantly correlated with the size of copepod ($p > 0.05$). Open symbols: active feeders that forage with feeding current or during cruising; Solid symbols: passive feeders that perform ambush feeding. The solid star represents female *O. davisae* in the present study.

tions in which *O. davisae* appears to be much more sensitive to turbulence than other copepods (SAIZ *et al*., 2003). The long antennae (about one body length) and setae may enable female *O. davisae* to detect weak deformation of flow (FIELDS, 2014).

Female *O. davisae*, as a strict ambush-feeding copepod (SAIZ *et al*., 2014), escaped at relatively weaker hydromechanical signals in contrast to almost all active-feeders (feeding-current or cruising feeder) reported in literatures (Fig. 8). Several larger ambush-feeding copepods (*e. g. Acartia tonsa, Calanus finmarchicus*, and *Tortanus discaudatus*) can initiate escapes at even lower signal levels than female *O. davisae*. In general, ambush-feeding copepods perform escapes at relatively lower signal levels than active-feeders with similar sizes (Fig. 8). This may explain partially why the predation risks for ambush-feeding copepods are up to one order of magnitude lower than active-feeding copepods (EIANE and OHMAN, 2004; THOR *et al*., 2008; VAN SOMMEREN GRÉVE *et al*., 2017).

Response strategy

Jumps against hydromechanical signals were faster and longer than those in still water. All jumps triggered by hydromechanical signals were clearly directed towards lower-deformation regions. Therefore, it is likely that female *O. davisae* wants to leave environments with deformation rate exceeding a certain level ($0.1\ s^{-1}$). Compared with other copepod species using the parameter "jump distance scaled by body length (BL)," female *O. davisae* jumped shorter distances (around 2 BL) (BURDICK *et al*., 2007; WAGGETT and BUSKEY, 2007). However, with these highly directional jumps against hydromechanical stim-

uli, female *O. davisae* can reach regions of relatively calmer conditions. It reflects that female *O. davisae* can discriminate not only the strength but also the directional information of flow fields. This finding is consistent with field observations, showing that *Oithona* copepods tend to avoid high-turbulence layers (SAIZ *et al.*, 2003). High-turbulence conditions increase the predator-prey encounter rate (GILBERT and BUSKEY, 2005), which will result in higher vulnerability, as has been observed in *A. tonsa* with blenny fish (CLARKE *et al.*, 2005) and blue mussel (JONSSON *et al.*, 2009) as predators. Therefore, to seek a refuge less accessible to predators may be an effective way to decrease the predation risks for small and rather slow copepods like *O. davisae* (PASTERNAK *et al.*, 2006).

Because copepods have less chances to survive short distance attacks from relatively large predators, encounter prevention becomes a better strategy than active attempts to escape (PASTERNAK *et al.*, 2006). Female *O. davisae* spends most of time (90–98%) in sinking, which is usually thought to reduce self-generated signals, and consequently minimize the detection probability by mechanoreceptive predators (KIØRBOE and VISSER, 1999; TITELMAN, 2001; JIANG and PAFFENHÖFER, 2004; BRADLEY *et al.*, 2013). Because the Reynolds numbers generated during swimming were low (0.15 during sinking and 1.03 during jump), the self-generated signals (Δ', s^{-1}) in front of female *O. davisae* can be evaluated by assuming the copepod as a Stokes' sphere (KIØRBOE and VISSER, 1999):

$$\Delta' = \frac{3Uc(R^2 - c^2)}{2R^4} \quad (4),$$

where U (mm s^{-1}) is the moving speed, c (mm) is the radius of copepod, and R (mm) is the distance to the center of copepod. According to our calculation, the deformation rate generated by

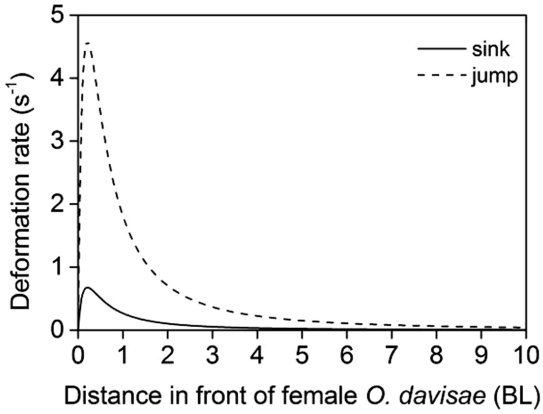

Fig. 9 Deformation rates generated in front of female *O. davisae* during its sinking and jump processes. The copepod was assumed to be a Stokes' sphere with diameter of 0.41 mm. The sinking and jump speeds were 0.37 mm s^{-1} and 2.51 mm s^{-1}, respectively. The Reynolds number was 0.15 during sinking and 1.03 during jump.

sinking accounts for only 15% of that by jump (Fig. 9). Therefore, female *O. davisae* can effectively suppress self-generated signals during sinking. It can help reduce the detection probability by mechanoreceptive predators, and at the same time, decrease interferences to its own predator detection.

Less self-generated "noise" can also decrease interference to the detection of motile prey. We calculated the hydromechanical signal level for prey detection of *O. davisae* by referring to its foraging experiment (with equation 4). It was reported that *O. davisae* can detect *T. tetrathele* (radius of 6 μm, moving speed of 0.2 mm s^{-1}) at 0.12 ± 0.05 mm in front of the first antennae (CHENG *et al.*, 2014). According to our calculation, the hydromechanical stimulus generated by *T. tetrathele* to trigger foraging behavior of female *O. davisae* was 0.06–0.31 (0.11 ± 0.05) s^{-1}. Under the given deformation threshold (0.11 s^{-1}) for prey detection, prey perception of female *O. davisae* can be interfered by its own jump to as far

as 6 BL from body surface; however, the interference during sinking was limited to less than 2 BL. Therefore, a long sinking time (around 95%) may be an ideal strategy for *O. davisae* that is hydromechanically-sensitive (PAFFENHÖFER and MAZZOCCHI, 2002).

Individual-level variability

We found that swimming behaviors of female *O. davisae* varied significantly between individuals under both "still water" and "suction flow" conditions. Despite the little knowledge of individual specialization in copepods, the inter-individual variability in behavior can be even higher in nature because of the differences in gender, age, and size, as well the existence of different preys, predators or mates (SEURONT *et al*., 2004). Such a big variation may also result from the fact that, in constantly changing marine environment, even individuals of the same copepod species may encounter different hydromechanical stimuli (derived from background turbulence or swimming organisms). A high intra- and inter-individual variability in escape behavior may raise the difficulties for predators to learn and develop an advanced strategy to forage on a specific species of copepods.

Conclusions

The behavioral responses of individual female *O. davisae* to hydromechanical stimuli were studied quantitatively. In absence of hydromechanical stimulus, female *O. davisae* normally jumps 0.3 mm (0.7 BL) at speed of 2.4 mm s^{-1} (6 BL s^{-1}); however, when the deformation rate exceeds 0.1 s^{-1}, it can escape over 0.8 mm (2 BL) with speed of 5.9 mm s^{-1} (15 BL s^{-1}). We assume that female *O. daivsae* escapes with higher jump speed and longer jump distance under high-deformation conditions because the normal jump may not be enough to survive potential predation risks.

The deformation rate that triggers female *O. davisae* to escape ranges widely (0.1–1.9 s^{-1}). In response to hydromechanical stimulus, female *O. davisae* jumps towards lower-deformation conditions most of time. It infers that female *O. davisae* can discriminate not only the strength but also the directional information of flow fields. Our results also suggest that female *O. davisae* prefers a calm environment where the local deformation rate is smaller than 0.1 s^{-1}. In relation to the low deformation level for prey detection, adult female *O. davisae* is easily interfered by turbulence (KIØRBOE and SAIZ, 1995; SAIZ *et al*., 2003); and therefore, a quiescent environment with low turbulence intensity can be beneficial to detect prey.

The observation of single copepods facilitated the characterization of a high intra- and inter-individual variability in behavioral responses. It reveals that copepods are a group of organisms with a variety of individual characteristics (even for the same species and similar size). Since hydromechanical signals of flow fields are used in many tasks (*e. g.* foraging, mating, predator avoidance) of the life history of copepods, the individual-level variability in the behavioral responses may have important consequences not only for the copepod population dynamics but also for the entire ecosystem functioning.

Acknowledgements

This work was supported by the Sasakawa Scientific Research Grant (26–742) from The Japan Science Society. JML was supported by a postdoctoral fellowship from the Japan Society for Promotion of Science (PE16401). We thank Dr. Takuo Omura for providing *T. tetrathele* in the culture of copepods.

References

BRADLEY, C. J., J. R. STRICKLER, E. J. BUSKEY and P. H. LENZ (2013): Swimming and escape behavior in two species of calanoid copepods from nauplius to adult. Journal of Plankton Research, **35**, 49–65.

BURDICK, D. S., D. K. HARTLINE and P. H. LENZ (2007): Escape strategies in co-occurring calanoid copepods. Limnology and Oceanography, **52**, 2373–2385.

BUSKEY, E. J., K. S. BAKER, R. C. SMITH and E. SWIFT (1989): Photosensitivity of the oceanic copepods *Pleuromamma gracilis* and *Pleuromamma xiphias* and its relationship to light penetration and daytime depth distribution. Marine Ecology Progress Series, **55**, 207–216.

CEBALLOS, S. and T. KIØRBOE (2011): Senescence and sexual selection in a pelagic copepod. PLoS ONE, **6**, e18870.

CHENG, W. T., T. AKIBA, T. OMURA and Y. TANAKA (2014): On the foraging and feeding ability of *Oithona davisae* (Crustacea, Copepoda). Hydrobiologia, **741**, 167–176.

CLARKE, R. D., E. J. BUSKEY and K. C. MARSDEN (2005): Effects of water motion and prey behavior on zooplankton capture by two coral reef fishes. Marine Biology, **146**, 1145–1155.

EIANE, K. and M. D. OHMAN (2004): Stage-specific mortality of *Calanus finmarchicus*, *Pseudocalanus elongatus* and *Oithona similis* on Fladen Ground, North Sea, during a spring bloom. Marine Ecology Progress Series, **268**, 183–193.

FERRARI, F. D. and J. ORSI (1984): *Oithona davisae*, new species, and *Limnoithona sinensis* (Burckhardt, 1912) (Copepoda: Oithonidae) from the Sacramento-San Joaquin Estuary, California. Journal of Crustacean Biology, **4**, 106–126.

FIELDS, D. M. (2000): Characteristics of the high frequency escape reactions of *Oithona* sp. Marine and Freshwater Behaviour and Physiology, **34**, 21–35.

FIELDS, D. M. (2014): The sensory horizon of marine copepods. *In* Copepods: Diversity, Habitat and Behavior. SEURONT, L. (eds.), Nova Science Publishers, p. 157–179.

FIELDS, D. M. and J. YEN (1997): The escape behavior of marine copepods in response to a quantifiable fluid mechanical disturbance. Journal of Plankton Research, **19**, 1289–1304.

FIELDS, D. M., D. S. SHAEFFER and M. J. WEISSBURG (2002): Mechanical and neural responses from the mechanosensory hairs on the antennule of *Gaussia princeps*. Marine Ecology Progress Series, **227**, 173–186.

FIELDS, D. M., S. D. SHEMA, H. I. BROWMAN, T. Q. BROWNE and A. B. SKIFTESVIK (2012): Light primes the escape response of the calanoid copepod, *Calanus finmarchicus*. PLoS ONE, **7**, e39594.

GILBERT, O. M. and E. J. BUSKEY (2005): Turbulence decreases the hydrodynamic predator sensing ability of the calanoid copepod *Acartia tonsa*. Journal of Plankton Research, **27**, 1067–1071.

JAKOBSEN, H. H. (2001): Escape response of planktonic protists to fluid mechanical signal. Marine Ecology Progress Series, **214**, 67–78.

JIANG, H. S. and T. R. OSBORN (2004): Hydrodynamics of copepods: a review. Surveys in Geophysics, **25**, 339–370.

JIANG, H. S. and G. A. PAFFENHÖFER (2004): Relation of behavior of copepod juveniles to potential predation by omnivorous copepods: an empirical-modeling study. Marine Ecology Progress Series, **278**, 225–239.

JONSSON, A., T. G. NIELSEN, I. HRUBENJA, M. MAAR and J. K. PETERSEN (2009): Eating your competitor: functional triangle between turbulence, copepod escape behavior and predation from mussels. Marine Ecology Progress Series, **376**, 143–151.

KIØRBOE, T. (2013): Attack or attacked: the sensory and fluid mechanical constraints of copepods' predator-prey interactions. Integrative and Comparative Biology, **53**, 821–831.

KIØRBOE, T. and E. SAIZ (1995): Planktivorous feeding in calm and turbulent environments, with emphasis on copepods. Marine Ecology Progress Series, **122**, 135–145.

KIØRBOE, T. and A. W. VISSER (1999): Predator and prey perception in copepods due to hydromechanical signals. Marine Ecology Progress Series, **179**, 81–95.

KIØRBOE, T., E. SAIZ and A. VISSER (1999): Hydrody-

namic signal perception in the copepod *Acartia tonsa*. Marine Ecology Progress Series, **179**, 97–111.

Lenz, P. H. and D. K. Hartline (1999): Reaction times and force production during escape behavior of a calanoid copepod, *Undinula vulgaris*. Marine Biology, **133**, 249–258.

Paffenhöfer, G. A. and M. G. Mazzocchi (2002): On some aspects of the behavior of *Oithona plumifera* (Copepoda: Cyclopoida). Journal of Plankton Research, **24**, 129–135.

Pasternak, A. F., V. N. Mikheev and J. Wanzenböck (2006): How plankton copepods avoid fish predation: from individual responses to variations of the life cycle. Journal of Ichthyology, **46**, 220–226.

Saiz, E., A. Calbet and E. Broglio (2003): Effects of small-scale turbulence on copepods: The case of *Oithona davisae*. Limnology and Oceanography, **48**, 1304–1311.

Saiz, E., K. Griffell, A. Calbet and S. Isari (2014): Feeding rates and prey: predator size ratios of the nauplii and adult females of the marine cyclopoid copepod *Oithona davisae*. Limnology and Oceanography, **59**, 2077–2088.

Seuront, L., J. S. Hwang, L. C. Tseng, F. G. Schmitt, S. Souissi and C. K. WONG (2004): Individual variability in the swimming behavior of the subtropical copepod *Oncaea venusta* (Copepoda: Poecilostomatoida). Marine Ecology Progress Series, **283**, 199–217.

Strickler, J. R. and A. K. Bal (1973): Setae on the first antennae of the copepod *Cyclops scutifer* (Sars): their structure and importance. Proceedings of the National Academy of Sciences of the United States of America, **70**, 2656–2659.

Thor, P., T. G. Nielsen and P. Tiselius (2008): Mortality rates of epipelagic copepods in the post-spring bloom period in Disko Bay, western Greenland. Marine Ecology Progress Series, **359**, 151–160.

Titelman, J. (2001): Swimming and escape behavior of copepod nauplii: implications for predator-prey interactions among copepods. Marine Ecology Progress Series, **213**, 203–213.

Uye, S. and K. Sano (1995): Seasonal reproductive biology of the small cyclopoid copepod *Oithona davisae* in a temperate eutrophic inlet. Marine Ecology Progress Series, **118**, 121–128.

van Sommeren Gréve, H., R. Almeda and T. Kiørboe (2017): Motile behavior and predation risk in planktonic copepods. Limnology and Oceanography, **62**, 1810–1824.

Viitasalo, M., T. Kiørboe, J. Flinkman, L. W. Pedersen and A. W. Visser (1998): Predation vulnerability of planktonic copepods: consequences of predator foraging strategies and prey sensory abilities. Marine Ecology Progress Series, **175**, 129–142.

Visser, A. W. (2001): Hydromechanical signals in the plankton. Marine Ecology Progress Series, **222**, 1–24.

Waggett, R. J. and E. J. Buskey (2007): Copepods escape behavior in non-turbulent and turbulent hydrodynamic regimes. Marine Ecology Progress Series, **334**, 193–198.

Woodson, C. B., D. R. Webster and A. C. True (2014): Copepod behavior: oceanographic cues, distributions and trophic interactions. *In* Copepods: Diversity, Habitat and Behavior. Seuront, L. (eds.), Nova Science Publishers, p. 215–253.

Yen, J., P. H. Lenz, D. V. Gassie and D. K. Hartline (1992): Mechanoreception in marine copepods: electrophysiological studies on the first antennae. Journal of Plankton Research, **14**, 495–512.

Received: December 27, 2017
Accepted: January 27, 2018